

Synthesis, Structures, and Magnetic Properties of Doubly Face-Sharing Heterotrinuclear Ni^{II}–Ln^{III}–Ni^{II} (Ln = Eu, Gd, Tb, and Dy) Complexes

Tomoka Yamaguchi,[1] Yukinari Sunatsuki,[1] Hiroyuki Ishida,[1] Masaaki Kojima,*[1] Haruo Akashi,[2] Nazzareno Re,[3] Naohide Matsumoto,[4] Andrzej Pochaba,[5] and Jerzy Mroziński[5]

[1]Department of Chemistry, Faculty of Science, Okayama University, 3-1-1 Tsushima-naka, Okayama 700-8530

[2]Research Institute of Natural Sciences, Okayama University of Science, Ridai-cho, Okayama 700-0005

[3]Facolta di Farmacià, Universita degli Studi "G. D'Annunzio," I-66100 Chieti, Italy

[4]Department of Chemistry, Faculty of Science, Kumamoto University, Kumamoto 860-8555

[5]Faculty of Chemistry, University of Wrocław, 14 F. Joliot-Curie, 50-383 Wrocław, Poland

Received December 5, 2007; E-mail: kojima@cc.okayama-u.ac.jp

Heterotrinuclear $[(Ni^{II}L)_2Ln^{III}(NO_3)]$ complexes (where H_3L = 1,1,1-tris[(salicylideneamino)methyl]ethane and Ln = Gd (**1**), Eu (**2**), Tb (**3**), and Dy (**4**)) were prepared by treating $[Ni(H_{1.5}L)]Cl_{0.5}$ with $Ln(NO_3)_3 \cdot 6H_2O$ in the presence of triethylamine. Complexes $\mathbf{1} \cdot 2CH_3OH$, $\mathbf{3} \cdot 2CH_3OH$, and $\mathbf{4} \cdot C_2H_5OH \cdot 0.5H_2O$ crystallized in the triclinic space group, $P\bar{1}$ (No. 2), with $Z = 2$, while $\mathbf{2} \cdot CH_3OH \cdot 0.5H_2O$ crystallized in the tetragonal space group, $I4_1/a$ (No. 88), with $Z = 8$. All the complexes had very similar structures. Each complex was a doubly face-sharing trinuclear molecule. The Ni^{II} ion is coordinated by the L^{3-} ligand in an N_3O_3 coordination sphere, and the three phenolate oxygen atoms coordinate to an Ln^{III} ion as bridging atoms. The Ln^{III} ion is eight coordinate with six phenolate oxygen atoms of the two L^{3-} ligands and two oxygen atoms of NO_3^-. Coordination of the NO_3^- group entails a bending of the Ni···Ln···Ni angle (ca. 140°). All the complexes involve π–π and CH–π interactions between the neighboring molecules to form a three-dimensional structure. Temperature-dependent magnetic susceptibility and field-dependent magnetization measurements on **1** showed a ferromagnetic interaction between the Ni^{II} and Gd^{III} atoms. A ferromagnetic interaction was also suggested for Ni^{II}–Tb^{III} (**3**) and Ni^{II}–Dy^{III} (**4**).

Heterometallic 3d–4f complexes have attracted much attention in fields such as luminescence,[1] MOCVD,[2] and single molecule magnets (SMMs).[3] To develop these studies further, it is necessary to evolve synthetic procedures, and control of the nuclearity of the complex is particularly important. Recently, we have prepared di-, tri-, and tetranuclear Ni^{II}–Gd^{III} complexes using the "complexes-as-ligands" strategy, and we found that we could control the nuclearity of such complexes by selecting an additional ligand on the Gd^{III} ion.[4]

We are interested in creating SMMs comprised of 3d–4f systems. Lanthanide (Ln) metal ions have a large ground state spin and a strong easy axis magnetic anisotropy, and the magnetic interactions of many 3d–4f complexes have been reported to be ferromagnetic. All these properties are favorable for 3d–4f complexes behaving as SMMs. Polynuclear 3d–4f complexes will meet the requirement to be identified as SMMs by a smaller number of metal ions than the 3d-transition metal clusters. Recently, we have observed that the heterodinuclear Ni^{II}–Dy^{III} complex, $[NiLDy(hfac)_2]$ (where H_3L = 1,1,1-tris[(salicylideneamino)methyl]ethane, Chart 1; Hhfac = hexafluoroacetylacetone), displays a frequency dependence of the out-of-phase component (χ_M'') characteristic of SMMs.[5] However, the blocking temperature, T_B, was below 2 K, and we did not observe any hysteresis in the magnetization of this sample. It is natural to expect that Ni^{II}–Ln^{III}–Ni^{II}-type heterotrinuclear complexes will more easily satisfy the conditions for SMMs,

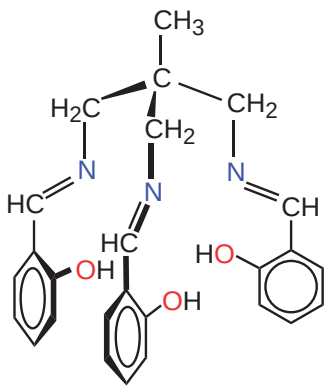

Chart 1. Structure of the H_3L ligand.

and we initiated a study along this line. Especially, we were interested in the magnetic properties of Tb and Dy complexes, because most of the 3d–4f complexes behaving as SMMs involve the Tb^{III} and Dy^{III} ions. In this paper, we report on the structure and magnetic properties of trinuclear $[(Ni^{II}L)_2Ln^{III}(NO_3)]$ complexes (where Ln = Eu, Gd, Tb, and Dy). Part of this work has been reported in another publication.[4] Very recently, Shiga et al.[6] described the magnetic properties of Ni^{II}–Ln^{III}–Ni^{II}-type heterotrinuclear complexes of 2,6-di(acetoacetyl)pyridine.

Published on the web May 14, 2008; doi:10.1246/bcsj.81.598

Table 1. Crystallographic Data for $[(NiL)_2Gd(NO_3)]\cdot 2CH_3OH$ (**1**·$2CH_3OH$), $[(NiL)_2Eu(NO_3)]\cdot CH_3OH\cdot 0.5H_2O$ (**2**·$CH_3OH\cdot 0.5H_2O$), $[(NiL)_2Tb(NO_3)]\cdot 2CH_3OH$ (**3**·$2CH_3OH$), and $[(NiL)_2Dy(NO_3)]\cdot C_2H_5OH\cdot 0.5H_2O$ (**4**·$C_2H_5OH\cdot 0.5H_2O$)

	1·$2CH_3OH$	**2**·$CH_3OH\cdot 0.5H_2O$	**3**·$2CH_3OH$	**4**·$C_2H_5OH\cdot 0.5H_2O$
Formula	$C_{54}H_{56}GdN_7Ni_2O_{11}$	$C_{53}H_{53}EuN_7Ni_2O_{10.5}$	$C_{54}H_{56}N_7Ni_2O_{11}Tb$	$C_{54}H_{55}DyN_7Ni_2O_{10.5}$
Formula weight	1253.73	1225.40	1255.40	1249.97
Crystal system	triclinic	tetragonal	triclinic	triclinic
Space group	$P\bar{1}$ (No. 2)	$I4_1/a$ (No. 88)	$P\bar{1}$ (No. 2)	$P\bar{1}$ (No. 2)
a/Å	13.2245(5)	17.3387(8)	13.2380(8)	14.0750(2)
b/Å	13.8535(4)	17.3387(8)	13.9498(7)	14.1625(2)
c/Å	16.4979(5)	37.3322(18)	16.4513(5)	16.3584(7)
α/°	90.290(2)	90	90.2050(16)	73.773(5)
β/°	104.022(2)	90	104.075(2)	89.486(2)
γ/°	111.761(1)	90	111.6407(18)	67.7941(5)
V/Å^3	2708.3(2)	11223.2(9)	2724.4(2)	2881.54(14)
Z	2	8	2	2
D_{calcd}/g cm^{-3}	1.537	1.450	1.530	1.441
μ/cm^{-1}	19.670	18.268	20.302	19.922
R_1[a] [$I > 2.0\sigma(I)$]	0.0522	0.0408	0.0539	0.0643
wR_2[b] [all data]	0.1316	0.1264	0.1510	0.1736
T/°C	−180	0	−180	−180

a) $R_1 = \Sigma||F_o| - |F_c||/\Sigma|F_o|$. b) $wR_2 = [\Sigma(w(F_o^2 - F_c^2)^2/\Sigma wF_o^2)^2]^{1/2}$.

Results and Discussion

Synthesis and Structure of Complexes 1–4. Complexes **1**–**4** were prepared by treating $[Ni(H_{1.5}L)]Cl_{0.5}$ with $Ln(NO_3)_3\cdot 6H_2O$ in the presence of triethylamine and isolated as pale green (**1**·$2CH_3OH$ and **2**·$CH_3OH\cdot 0.5H_2O$) or red (**3**·$2CH_3OH$ and **4**·$C_2H_5OH\cdot 0.5H_2O$) rhombic plates. They are efflorescent and easily lose solvent (methanol, ethanol, or water) molecules of crystallization, during which their color turns to a dull greenish brown. To investigate the magnetic properties of **2**–**4** that have the complicating effect of spin–orbit coupling,[7] we tried to prepare analogous Zn^{II}–Ln^{III} complexes, $[(Zn^{II}L)_2Ln^{III}(NO_3)]$ using a similar procedure to that used for **1**–**4**. Despite our efforts, we could not prepare any analogous Zn complexes. For example, the reaction of $[ZnL]^-$ with $Ln(NO_3)_3\cdot 6H_2O$ yielded only the homometal trinuclear Zn^{II}–Zn^{II}–Zn^{II}-type complex, $[Zn_3L_2]$.[8] The difference in reactivity between $[NiL]^-$ and $[ZnL]^-$ with $Ln(NO_3)_3\cdot 6H_2O$ may be related to the difference in ionic radius, 0.83 Å for six-coordinated Ni^{2+} versus 0.88 Å for six-coordinated Zn^{2+}.[9]

Complexes **1**·$2CH_3OH$, **3**·$2CH_3OH$, and **4**·$C_2H_5OH\cdot 0.5H_2O$ crystallize in the triclinic space group, $P\bar{1}$ (No. 2) with $Z = 2$, while **2**·$CH_3OH\cdot 0.5H_2O$ crystallizes in the tetragonal space group, $I4_1/a$ (No. 88) with $Z = 8$. The crystallographic data of **1**–**4** are listed in Table 1. The coordinate bond lengths, Ni···Ln distances, Ni···Ni distances, and Ni···Ln···Ni angles, along with their estimated standard deviation given in parentheses for **1**·$2CH_3OH$, **3**·$2CH_3OH$, and **4**·$C_2H_5OH\cdot 0.5H_2O$ are listed in Table 2, while similar values for **2**·$CH_3OH\cdot 0.5H_2O$ are listed in Table 3. All the complexes have a similar structure, and **1**·$2CH_3OH$ and **3**·$2CH_3OH$ are isomorphous with one another. We will describe the structure of **1**·$2CH_3OH$ as a representative example. The crystal structure consists of one $[(NiL)_2Gd(NO_3)]$ and two methanol molecules as an asymmetric unit. Figure 1a shows the molecular structure of **1**·$2CH_3OH$, along with the selected numbering scheme. The hydrogen atoms and methanol molecules have been omitted

Table 2. The Coordinate Bond Lengths (Å), Intermetallic Distances (Å), and Angles (°) with the Estimated Standard Deviation (in Parentheses) for $[(NiL)_2Gd(NO_3)]\cdot 2CH_3OH$ (**1**·$2CH_3OH$), $[(NiL)_2Tb(NO_3)]\cdot 2CH_3OH$ (**3**·$2CH_3OH$), and $[(NiL)_2Dy(NO_3)]\cdot C_2H_5OH\cdot 0.5H_2O$ (**4**·$C_2H_5OH\cdot 0.5H_2O$)

	1·$2CH_3OH$	**3**·$2CH_3OH$	**4**·$C_2H_5OH\cdot 0.5H_2O$
	Coordinate bond length/Å		
Ln(1)–O(1) (II)[a]	2.457(4)	2.444(4)	2.451(5)
Ln(1)–O(2) (III)[a]	2.275(4)	2.265(4)	2.260(6)
Ln(1)–O(3) (I)[a]	2.372(4)	2.375(4)	2.367(5)
Ln(1)–O(4) (I)[a]	2.365(3)	2.363(4)	2.360(5)
Ln(1)–O(5) (II)[a]	2.441(4)	2.435(5)	2.471(6)
Ln(1)–O(6) (III)[a]	2.291(3)	2.279(4)	2.276(5)
Ln(1)–O(7)	2.499(3)	2.463(4)	2.463(6)
Ln(1)–O(8)	2.480(4)	2.490(4)	2.477(5)
Ni(1)–O(1)	2.117(4)	2.119(5)	2.126(6)
Ni(1)–O(2)	2.084(4)	2.086(5)	2.081(7)
Ni(1)–O(3)	2.074(3)	2.063(3)	2.052(4)
Ni(1)–N(1)	2.039(6)	2.050(6)	2.043(9)
Ni(1)–N(2)	2.057(4)	2.068(5)	2.061(7)
Ni(1)–N(3)	2.069(4)	2.066(5)	2.070(7)
Ni(2)–O(4)	2.085(3)	2.080(4)	2.082(5)
Ni(2)–O(5)	2.143(3)	2.141(4)	2.139(5)
Ni(2)–O(6)	2.072(4)	2.066(5)	2.064(7)
Ni(2)–N(4)	2.057(4)	2.052(4)	2.066(6)
Ni(2)–N(5)	2.032(5)	2.038(6)	2.022(9)
Ni(2)–N(6)	2.068(5)	2.066(5)	2.075(8)
	Intermetallic distance/Å		
Ln(1)···Ni(1)	3.1670(7)	3.1647(8)	3.1451(11)
Ln(1)···Ni(2)	3.1703(6)	3.1632(7)	3.1599(10)
Ni(1)···Ni(2)	5.9539(6)	5.9464(10)	5.9406(14)
	Angle/°		
Ni(1)···Ln(1)···Ni(2)	139.935(19)	140.01(2)	140.831(3)

a) I, II, and III denote Group I, Group II, and Group III, respectively, of the Ln–O(phenolate) bonds (see text for definition).

Table 3. The Coordinate Bond Lengths (Å), Intermetallic Distances (Å), and Angle (°) with the Estimated Standard Deviation (in Parentheses) for $[(NiL)_2Eu(NO_3)]\cdot CH_3OH\cdot 0.5H_2O$ (**2**·$CH_3OH\cdot 0.5H_2O$)

Coordinate bond length/Å	
Eu(1)–O(1) (II)[a)]	2.481(3)
Eu(1)–O(2) (I)[a)]	2.376(3)
Eu(1)–O(3) (III)[a)]	2.288(2)
Eu(1)–O(4)	2.511(3)
Eu(1)–N(4)	2.912(5)
Ni(1)–O(1)	2.116(3)
Ni(1)–O(2)	2.068(2)
Ni(1)–O(3)	2.094(3)
Ni(1)–N(1)	2.047(3)
Ni(1)–N(2)	2.047(3)
Ni(1)–N(3)	2.029(3)
Intermetallic distance/Å	
Eu(1)···Ni(1)	3.1549(4)
Ni(1)···Ni(1)[b)]	6.0171(5)
Angle/°	
Ni(1)···Eu(1)···Ni(1)[b)]	143.830(13)

a) I, II, and III denote Group I, Group II, and Group III, respectively, of the Ln–O(phenolate) bonds (see text for definition). b) $1-x$, $1/2-y$, z.

for clarity. A view of the $N_3Ni(\mu\text{-}O)_3Gd(NO_3)(\mu\text{-}O)_3NiN_3$ core is shown in Figure 1b. Each Ni^{II} ion is coordinated by an L^{3-} ligand in an N_3O_3 coordination sphere, and the three phenolate oxygen atoms coordinate to a central Gd^{III} ion as bridging atoms to form a doubly face-sharing trinuclear molecule. The Ni–N lengths for **1**·$2CH_3OH$ are almost the same (av. 2.054 Å) as the Ni–N lengths (av. 2.047 Å) for the starting mononuclear Ni^{II} complex.[10] On the other hand, on complexation with Gd^{III}, the Ni–O bond lengths (av. 2.096 Å) increase from those in the starting mononuclear Ni^{II} complex (av. 2.078 Å). The configuration around each Ni^{II} ion is chiral with either a Δ or a Λ configuration due to the screw coordination arrangement of the achiral tripodal ligand around the metal ion. When two chiral molecules associate, both homochiral (Δ–Δ or Λ–Λ) and heterochiral (Δ–Λ) pairs are possible. Both the Ni units shown in Figure 1a have the Δ configuration. Thus, this is a homochiral Δ–Δ pair. Examination of molecular models indicated that the heterochiral pair involved severe steric repulsion between the aromatic groups of the terminal Ni units. On the other hand, the homochiral pair does not involve such steric congestion. Since the complex crystallizes in a centrosymmetric space group, $P\bar{1}$, molecules with Δ–Δ and Λ–Λ pairs coexist in the crystal to form a racemic crystal. In other words, **1**·$2CH_3OH$ does not undergo spontaneous resolution. The coordination geometry around each Ni^{II} ion is distorted from a regular octahedron toward that of a trigonal prism. The trigonal twist angle, ϕ, as defined in Figure 2, is a measure of the degree of twisting (trigonal prism = 0° and octahedron = 60°).[11] Both the values of $\phi 1$ and $\phi 2$ for the terminal Ni1 and Ni2 ions were 45°. The values of ϕ are tabulated in Table 4, together with those of the other complexes. The

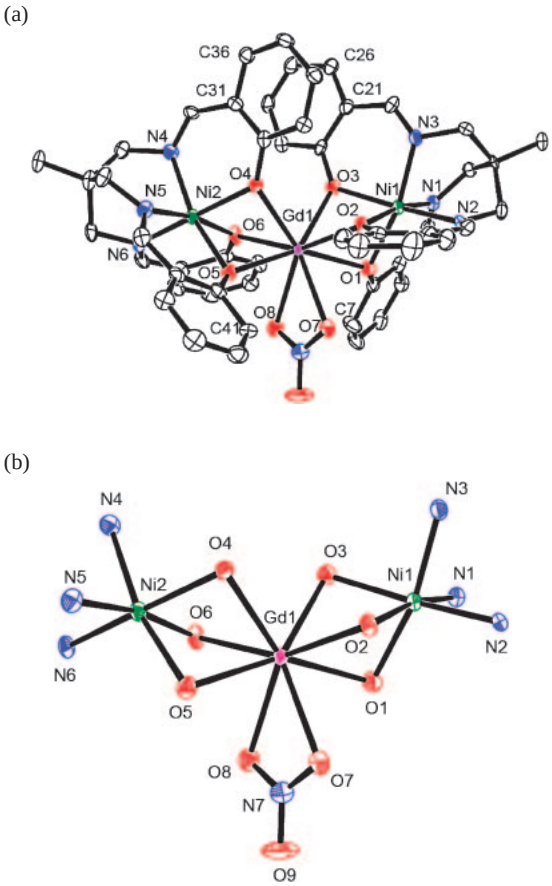

Figure 1. (a) ORTEP drawing of $[(NiL)_2Gd(NO_3)]\cdot 2CH_3OH$ (**1**), showing atom numbering and the 50% probability displacement ellipsoids. The hydrogen atoms and solvent molecules of crystallization are omitted for clarity. (b) A view of the $N_3Ni(\mu\text{-}O)_3Gd(NO_3)(\mu\text{-}O)_3NiN_3$ core.

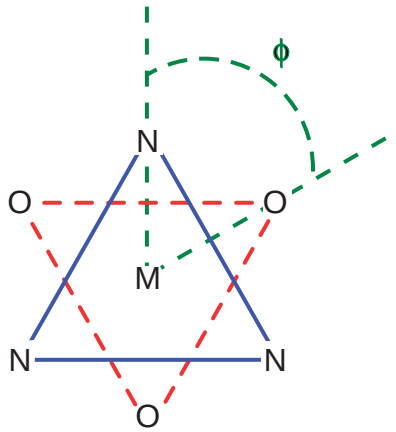

Figure 2. Definition of the trigonal twist angle, ϕ, a measure of the degree of twisting (trigonal prism = 0°, octahedron = 60°).

Gd^{III} ion is eight coordinate, with six phenolate oxygen atoms of the two L^{3-} ligands and two oxygen atoms of the NO_3^- taking part in the coordination. The dihedral angle between the two planes, defined by three phenolate oxygen atoms (O1, O2, and O3 and O4, O5, and O6) is 41.14° and the distance between the centroids is 3.361 Å. These data are also listed in

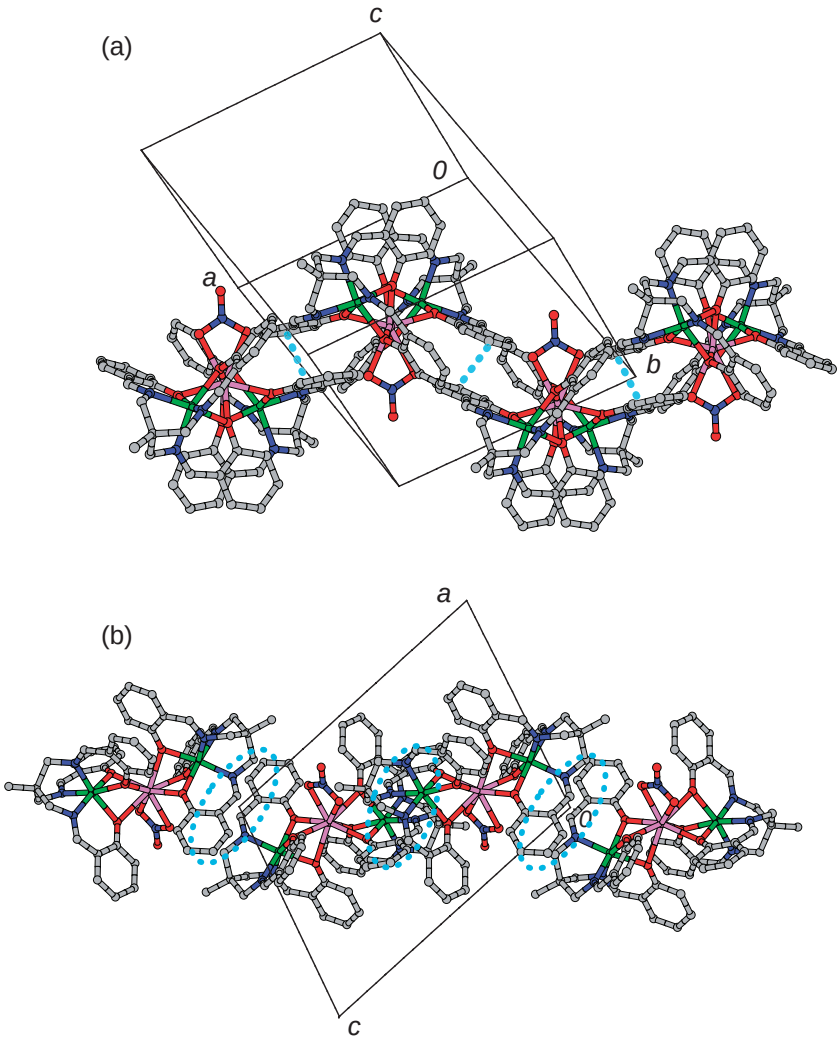

Figure 3. Crystal structure of $[(NiL)_2Gd(NO_3)]\cdot 2CH_3OH$ (**1**): (a) π–π stacking (light blue broken lines) forming a 1D chain structure along the [101] direction. (b) projection on the *ac* plane.

Table 4. Trigonal Twist Angle ϕ (°)[a)] and Dihedral Angle (°) between Two Planes Defined by Three Phenolate Oxygen Atoms, and Distance between Centroids[a)] for $[(NiL)_2Gd(NO_3)]\cdot 2CH_3OH$ (**1**·$2CH_3OH$), $[(NiL)_2Eu(NO_3)]\cdot CH_3OH\cdot 0.5H_2O$ (**2**·CH_3OH·$0.5H_2O$), $[(NiL)_2Tb(NO_3)]\cdot 2CH_3OH$ (**3**·$2CH_3OH$), and $[(NiL)_2Dy(NO_3)]\cdot C_2H_5OH\cdot 0.5H_2O$ (**4**·C_2H_5OH·$0.5H_2O$)

	$\phi 1$/°	$\phi 2$/°	Dihedral angle/°	Distance between the centroids/Å
1	45	45	41.14	3.361
2	43		37.83	3.404
3	43	44	40.45	3.352
4	44	43	40.23	3.364

a) See Figures 1 and 2, and text for definition.

Table 4 together with data for complexes **2**–**4**. There are three pairs of aromatic rings in the molecule, and one pair, Ring 1 (C21–C26) and Ring 2 (C31–C36), is π–π stacked, with the distance ca. 3.5 Å. The Gd–O (phenolate) bond length spans a wide range (2.275(4)–2.457(4) Å), and can be classified into three groups: Group I is for phenolate oxygen atoms attached to the π–π stacked rings (Gd1–O3 = 2.372(4) Å and Gd1–O4 = 2.365(3) Å); Group II is for oxygen atoms near the nitrate ions, and has the longest bond lengths (Gd1–O1 = 2.457(4) Å and Gd1–O5 = 2.441(4) Å); and Group III is for the rings situated between the other two groups, and has the shortest bond lengths (Gd1–O2 = 2.275(4) Å and Gd1–O6 = 2.291(3) Å). The differences in the Gd–O bond length seem to be related to the coordination of a nitrate ion. Coordination of a nitrate ion causes steric interaction with the neighboring benzene rings (Group II), O7···C41 = 3.101(8) Å and O8···C7 = 3.104(9) Å. Thus, the Gd1–O1 and Gd1–O5 bonds become longer to alleviate the steric congestion. In crystals of **1**·$2CH_3OH$, the Ni1···Gd1, Ni2···Gd1, and Ni1···Ni2 distances are 3.1670(7), 3.1703(6), and 5.9539(6) Å, respectively (Table 2).

In the crystal, adjacent molecules are connected by π–π stacking to form a one-dimensional (1D) chain structure along the [101] direction (Figure 3). The average π–π stacking distance is ca. 3.5 Å. A CH–π interaction exists between the chains along the *b* axis (Figure 4). The average CH–π distance is ca. 2.8 Å. The two methanol molecules of crystallization, and those created by a symmetry operation ($2-x$, $1-y$,

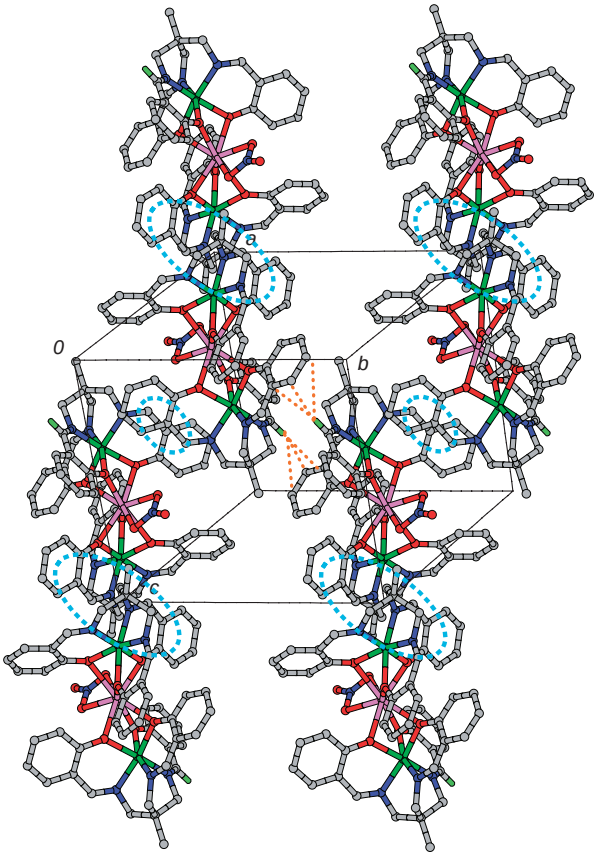

Figure 4. Crystal structure of $[(NiL)_2Gd(NO_3)]\cdot 2CH_3OH$ (**1**), showing π–π stacking (light blue broken line circles) and CH–π interaction (orange broken lines) between the chains along the *b* axis.

$1 - z$), are hydrogen bonded: O10···O11 = 2.782(9) Å, O11···$O10^{i}$ = 2.808(8) Å (Figure S1). There is also an interaction along the *a* axis through the hydrogen bonds between the methanol molecules and CH–π interaction between the chains (Figure S1) to form a three-dimensional structure. The smallest distances between the metal ions in the neighboring molecules are: Gd···Gd = 9.8606(4) Å, Ni···Ni = 6.5858(9) Å, and Gd···Ni = 7.7637(6) Å.

The crystal structure of $\mathbf{2}\cdot CH_3OH\cdot 0.5H_2O$ is different from the other structures. As Figure 5 shows, 1D chains are formed by π–π stacking along the *a* axis and *b* axis. The average π–π stacking distance is ca. 3.5 Å. The chains along the two directions are further connected by CH–π interactions to form a 3D structure (Figure S2). The average CH–π distance is ca. 2.8 Å. The shortest distances between the metal ions of neighboring molecules of $\mathbf{2}\cdot CH_3OH\cdot 0.5H_2O$ are: Eu···Eu = 9.67935(16) Å, Ni···Ni = 7.8866(6) Å, and Eu···Ni = 8.2418(5) Å.

It is relevant to compare the structures of **1**–**4**. The structural parameters about the two terminal Ni^{II} ions are similar to each other. The average Ln–O bond length (Eu (**2**) = 2.41 Å; Gd (**1**) = 2.40 Å; Tb (**3**) = 2.39 Å; and Dy (**4**) = 2.39 Å) depends on the size of the eight-coordinate lanthanide ion (Eu = 1.206 Å; Gd = 1.193 Å; Tb = 1.180 Å; and Dy = 1.167 Å).[9]

Magnetic Properties of 1–4. All the complexes are efflorescent, and they easily lose the solvent molecules of crystallization. The samples we used in our magnetic measurements

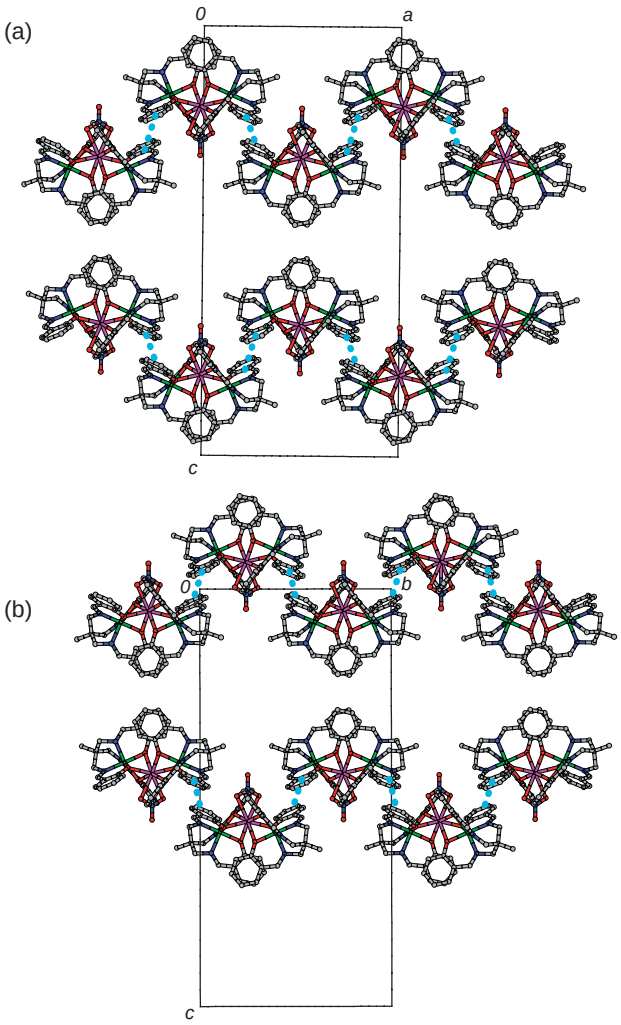

Figure 5. Crystal structure of $[(NiL)_2Eu(NO_3)]\cdot CH_3OH\cdot 0.5H_2O$ ($\mathbf{2}\cdot CH_3OH\cdot 0.5H_2O$): (a) 1D chains along the *a* axis formed by π–π stacking, and (b) 1D chains along the *b* axis formed by π–π stacking. The light blue broken lines show π–π stacking.

were formulated as $[(NiL)_2Ln(NO_3)]$ (see the Experimental section). Temperature-dependent molar susceptibility measurements on powdered samples were carried out in an applied field of 0.1 T in the temperature range 2–300 K. The data are represented in $\chi_M T$ versus T plots in Figure 6, where χ_M is the molar magnetic susceptibility and T is the absolute temperature. The value of $\chi_M T$ of **1** is 12.604 $cm^3\,K\,mol^{-1}$ at 300 K, which is larger than the value expected for two Ni^{II} ($S = 1$) and one Gd^{III} ($4f^7$, $J = 7/2$, $L = 0$, $S = 7/2$, $^8S_{7/2}$) noninteracting ions (9.875 $cm^3\,K\,mol^{-1}$). The profile of the curve for **1** is almost constant in the temperature range 50–300 K and shows a steady increase on reducing the temperature. The value of $\chi_M T$ increases rapidly below 10 K, indicating that the overall magnetic interaction between the metal ions is ferromagnetic. The maximum value of $\chi_M T$, 17.446 $cm^3\,K\,mol^{-1}$ at 2.0 K, is slightly smaller than the value of 17.875 $cm^3\,K\,mol^{-1}$ expected for an isolated $S = 11/2$ spin resulting from ferromagnetic coupling between the two Ni^{II} ($S = 1$) and Gd^{III} ($S = 7/2$) ions in a trinuclear complex. Fits to the exper-

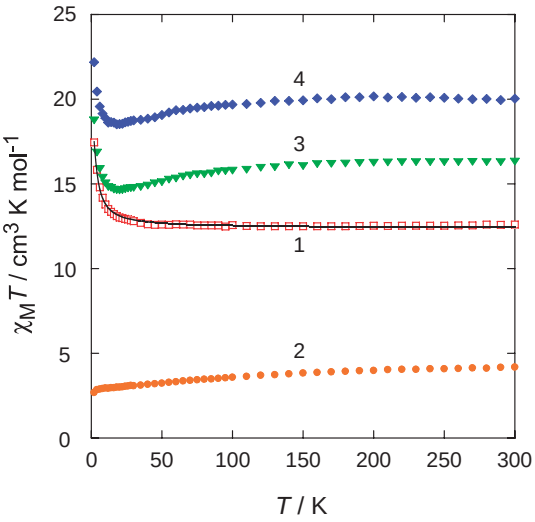

Figure 6. Magnetic behaviors of $[(NiL)_2Gd(NO_3)]$ (**1**, □), $[(NiL)_2Eu(NO_3)]$ (**2**, ●), $[(NiL)_2Tb(NO_3)]$ (**3**, ▼), and $[(NiL)_2Dy(NO_3)]$ (**4**, ◆) in the form of $\chi_M T$ versus T plots in the temperature range 2–300 K. The solid line corresponds to the best data fits for **1**.

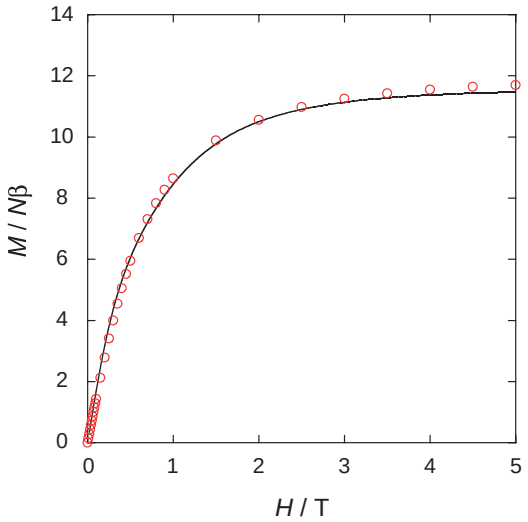

Figure 7. Field dependence of magnetization at 2 K for $[(NiL)_2Gd(NO_3)]$ (**1**). The solid line corresponds to the best data fit (cf. text).

imental data were performed assuming for the Gd^{III} ion an isotropic $^8S_{7/2}$ state without orbital angular momentum and using the following spin Hamiltonian, $\mathbf{H} = g\beta(\mathbf{S}_{Ni1} + \mathbf{S}_{Ni2} + \mathbf{S}_{Gd})H + D_{Ni}[\mathbf{S}^2_{Ni1z} + S(S+1)/3] + D_{Ni}[\mathbf{S}^2_{Ni2z} + S(S+1)/3] + 2J(\mathbf{S}_{Ni1}\cdot\mathbf{S}_{Gd} + \mathbf{S}_{Ni2}\cdot\mathbf{S}_{Gd})$ in which g is an average g-factor for the Gd^{III} and Ni^{II} ions, H the applied field, D_{Ni} the zero field splitting (ZFS) parameter for Ni^{II}, and J the Heisenberg coupling constant between each of the two Ni^{II} ions and the central Gd^{III} ion. The inclusion of the ZFS term for Ni^{II} is consistent with the analysis of the magnetization data (see later), and allows for an improved fit at low temperatures.[12] The best-fit parameters to the data were $g = 2.24$, J (Ni–Gd) $= +0.19$ cm^{-1}, and $D = +2.1$ cm^{-1}. The calculated J (Ni–Gd) value is lower than that of Costes et al.[13] for a Gd^{III}–Ni^{II} dinuclear complex with two phenoxo bridges, of $J = +3.6$ cm^{-1}, but is similar to the value observed by Chen et al.[14] for a Gd^{III}–Ni^{II} compound with three phenoxo bridges, $J = +0.56$ cm^{-1}, and to the value recently reported by Shiga et al. for a trinuclear $Ni^{II}Gd^{III}Ni^{II}$ complex derived from 2,6-di(acetoacetyl)-pyridine with two alkoxo bridges, $J = +0.79$ cm^{-1}.[6]

The field dependence of the magnetization at 2 K was also measured, and the M versus H curve is shown in Figure 7. The data are qualitatively reproduced by Brillouin curve for the $S = 11/2$ spin system, demonstrating that the spin ground state is derived from the ferromagnetic coupling between Ni^{II} ($S = 1$) and Gd^{III} ($S = 7/2$) ions. The data were well simulated (see the solid lines in Figure 7) including the ZFS for the same spin systems, and the best fit to the experimental data yielded the following values: $g = 2.06$ and $D = +0.15$ cm^{-1}. It is worth noting that the D value obtained from the fit of the magnetization data refers to the $S = 11/2$ state, and can be compared with the single ion values for Ni^{II} obtained from a fit of the magnetic susceptibility using the Wigner–Eckart theorem.[15] Accordingly, $D_{11/2}$ can be written as a weighted combination of $D_{Ni^{II}}$ and $D_{Gd^{III}}$, with a much larger weight of the latter term, and taking into account that $D_{Gd^{III}}$ is negligibly small, it follows that $D_{11/2} \ll D_{Ni^{II}}$. This justifies, at least qualitatively, the smaller value of D, by one order of magnitude, obtained from the fit of the magnetization data.

The magnetic data for **2**–**4** are also shown as plots of $\chi_M T$ versus T in Figure 6. The profiles of **3** and **4** are similar to each other. The $\chi_M T$ value of 16.32 cm^3 K mol^{-1} at 300 K for **3** is larger than the calculated value of 13.82 cm^3 K mol^{-1} for two independent Ni^{II} ($S = 1$) and Tb^{III} ($4f^8$, $J = 6$, $S = 3$, $L = 3$, $^7F_6$), and the $\chi_M T$ value was almost constant in the temperature range 100–300 K, and it decreases gradually with decreasing temperature to 14.61 cm^3 K mol^{-1} at 20 K, but then increases at lower temperatures reaching a maximum value of 18.75 cm^3 K mol^{-1} at 2 K. The $\chi_M T$ value of 20.03 cm^3 K mol^{-1} at 300 K for **4** is larger than the calculated value of 16.17 cm^3 K mol^{-1} for two independent Ni^{II} ($S = 1$) and Dy^{III} ($4f^9$, $J = 15/2$, $S = 5/2$, $L = 5$, $^6H_{15/2}$), and the $\chi_M T$ value was almost constant in the temperature range 100–300 K, and it decreases gradually with decreasing temperature to 18.51 cm^3 K mol^{-1} at 18 K, but then increases at lower temperatures reaching a maximum value of 22.19 cm^3 K mol^{-1} at 2 K. For **2**, the $\chi_M T$ value of 4.19 cm^3 K mol^{-1} at 300 K is lager than the calculated value of 2.00 cm^3 K mol^{-1} for two independent Ni^{II} ($S = 1$) and Eu^{III} ($4f^6$, $J = 0$, $S = 3$, $L = 3$, $^7F_0$), and the value of $\chi_M T$ decreases steadily as the temperature decreases to 2.69 cm^3 K mol^{-1} at 2 K.

It is difficult to study the magnetic properties of **2**–**4** because of complications from spin–orbit coupling. We evaluated the Ni^{II}–Ln^{III} magnetic interactions (where Ln = Eu, Tb, and Dy) of heterodinuclear complexes $[(NiL)Ln(hfac)_2]$ using an empirical approach developed by Costes et al.[7] and Kahn et al.[16] The magnetic susceptibilities were compared with those of the isostructural Zn^{II}–Ln^{III} complexes, $[(ZnL)Ln(hfac)_2]$ containing a diamagnetic Zn^{II} ion, so we could investigate the nature of the magnetic interactions between Ni^{II} and Ln^{III}.[5] Thus, we tried to prepare the analogous Zn^{II}–Ln^{III} complexes, $[(Zn^{II}L)_2Ln^{III}(NO_3)]$, using a similar procedure to that used for **1**–**4**. Despite our efforts, we could not prepare any analogous Zn complexes, and so we could not use the empirical method.

We paid attention to the similarity between the $\chi_M T$–T profiles of **1**–**4** and those of [(NiL)Ln(hfac)$_2$] (Ln = Eu, Gd, Tb, and Dy), although the $\chi_M T$ values of the trinuclear complexes are larger than those of the dinuclear complexes over the entire temperature range as expected. A ferromagnetic interaction was indicated in [(NiL)Ln(hfac)$_2$] (Ln = Tb and Dy), while the interaction was negligible in [(NiL)Eu(hfac)$_2$].[5] Since ferromagnetic interactions are suggested in **3** and **4** to occur and these complexes have high $\chi_M T$ values, we expected that these complexes would be good candidates for SMMs. One of the characteristics of an SMM is the observation of frequency dependence in the ac susceptibility signals, and we carried out ac susceptibility measurements on **3** and **4** in a 3.0 G ac field oscillating at 20–1000 Hz in the temperature range of 2.0–5.0 K. However, neither **3** nor **4** exhibited any frequency dependence in the ac susceptibility signals.

Conclusion

By using $[NiL]^-$ as the ligand-complex, heterotrinuclear complexes [(NiL)$_2$Ln(NO$_3$)] (Ln = Gd (**1**), Eu (**2**), Tb (**3**), and Dy (**4**)) were prepared. Complexes **1**–**4** are Ni^{II}–Ln^{III}–Ni^{II}-type trinuclear complexes with a bent Ni···Ln···Ni angle (ca. 140°). All complexes involve π–π and CH–π interactions between neighboring molecules to form a 3D structure. Temperature-dependent magnetic susceptibility and field-dependent magnetization measurements of **1** showed a ferromagnetic interaction between the Ni^{II} and Gd^{III} sites. Although the nature of the magnetic interactions between Ni^{II} and Ln^{III} (Eu, Tb, and Dy) was not clearly shown in **2**–**4**, ferromagnetic interactions are expected for **3** (Tb) and **4** (Dy) from data in relation to related complexes. That frequency dependence in the ac susceptibility signals was not observed in **3** and **4** seems to be related to the 3D structure of these complexes. We are now trying to eliminate the intermolecular interaction by introducing suitable substituents on the tripodal ligand. We expect that such a complex will easily satisfy the conditions for SMMs with a high-spin ground state and a magnetic anisotropy.

Experimental

Materials. All the reagents and solvents used in the syntheses were of reagent grade and were used without further purification. The H_3L ligand[17] and [Ni($H_{1.5}$L)]Cl$_{0.5}$[10] were prepared according to literature procedures.

[(NiL)$_2$Ln(NO$_3$)] (Ln = Gd (1), Eu (2), Tb (3), and Dy (4)). All these complexes were prepared using a similar method. A representative procedure is given for **1**. A methanol solution (5 mL) of Gd(NO$_3$)$_3$·6H$_2$O (0.014 g, 0.03 mmol) and a methanol solution (5 mL) of triethylamine (0.012 g, 0.12 mmol) were added to [Ni($H_{1.5}$L)]Cl$_{0.5}$ (0.029 g, 0.06 mmol) in methanol (10 mL). The mixture was left at room temperature to deposit pale green crystals. These were collected by filtration and dried in a desiccator over P_4O_{10}. The methanol molecules of crystallization were lost on drying. Yield: 0.023 g (64%). Anal. Calcd for $C_{52}H_{48}GdN_7Ni_2O_9$ = [(NiL)$_2$Gd(NO$_3$)]: C, 52.50; H, 4.06; N, 8.24%. Found: C, 52.10; H, 3.69; N, 8.16%. IR (KBr disk): ν(C=N) 1631; ν(N=O) 1473; ν(NO$_2$) 1302 cm^{-1}.

2: Yield: 80%. Anal. Calcd for $C_{52}H_{48}EuN_7Ni_2O_9$ = [(NiL)$_2$Eu(NO$_3$)]: C, 52.73; H, 4.08; N, 8.27%. Found: C, 52.44; H, 3.79; N, 8.36%. IR (KBr disk): ν(C=N) 1635; ν(N=O) 1473; ν(NO$_2$) 1300 cm^{-1}.

3: Yield: 43%. Anal. Calcd for $C_{52}H_{48}N_7Ni_2O_9Tb$ = [(NiL)$_2$Tb(NO$_3$)]: C, 52.42; H, 4.06; N, 8.23%. Found: C, 52.03; H, 3.90; N, 8.08%. IR (KBr disk): ν(C=N) 1633; ν(N=O) 1474; ν(NO$_2$) 1300 cm^{-1}.

4: Yield: 67%. Anal. Calcd for $C_{52}H_{48}DyN_7Ni_2O_9$ = [(NiL)$_2$Dy(NO$_3$)]: C, 52.27; H, 4.05; N, 8.20%. Found: C, 52.15; H, 3.81; N, 7.99%. IR (KBr disk): ν(C=N) 1634; ν(N=O) 14743; ν(NO$_2$) 1299 cm^{-1}.

Physical Measurements. Elemental analyses (C, H, and N) were performed using a Perkin-Elmer 2400II elemental analyzer. The IR spectra were recorded using a JASCO FT/IR FT-550 spectrophotometer, with the samples prepared as KBr disks. Magnetic susceptibility measurements were carried out using a Quantum Design MPMS 2 SQUID magnetometer (located at Okayama University) in the temperature range 2–300 K and under an applied magnetic field of 0.1 T. Magnetization versus magnetic field measurements were carried out using a Quantum Design MPMS-5SP SQUID magnetometer (located at Kumamoto University) at 2 K in the field range 0–5 T. For magnetic measurements, the samples were placed into a gelatin capsule, which was then placed inside a plastic straw. Pascal's constants were used to correct for diamagnetism.[15] The ac susceptibility measurements were carried out in a 3.0 G ac field oscillating at 20–1000 Hz in the temperature range of 2.0–5.0 K at the University of Wrocław.

X-ray Data Collection, Reduction, and Structure Determination. A suitable crystal obtained from an ethanol or a methanol solution was placed in a capillary tube with a small volume of mother liquid. The X-ray measurements were carried out using a Rigaku RAXIS-IV imaging plate area detector (located at the Okayama University of Science) employing graphite monochromated Mo Kα radiation (λ = 0.71069 Å). The structures were determined using direct methods (SHELXS97 or SIR97)[18] and expanded using Fourier techniques[19] and successive Fourier difference methods with a full-matrix least-squares refinement on F^2. The nonhydrogen atoms were refined anisotropically. Hydrogen atoms were refined using the riding model. All calculations were performed using the Crystal Structure 3.8 software package.[20] Crystallographic data for **1**–**4** have been deposited at the Cambridge Crystallographic Data Centre, Deposition numbers CCDC-676080, -676081, -676082, and -676083 for **1**, **2**, **3**, and **4**, respectively. Although the X-ray crystal structure analysis of **1** was carried out before and the crystallographic data were deposited as deposition number CCDC-229922,[4] we analyzed the structure using the same X-ray data and obtained more reliable results, and the data have been deposited as CCDC-676080. Copies of the data can be obtained free of charge via http://www.ccdc.cam.ac.uk/conts/retrieving.html (or from the Cambridge Crystallographic Data Centre, 12, Union Road, Cambridge, CB2 1EZ, UK; Fax: +44 1223 336033; e-mail: deposit@ccdc.cam.ac.uk).

This work was supported in part by a Grant-in-Aid for Scientific Research (Nos. 16205010, 16750050, and 17350028) from the Ministry of Education, Culture, Sports, Science and Technology, by the Iketani Science and Technology Foundation, and also by the EU 6FP MAGMANet Programme. T. Y. was supported by the JSPS program for Research Fellowships for Young Scientists (No. 17003601).

Supporting Information

Crystal structures of [(NiL)$_2$Gd(NO$_3$)] (**1**) (Figure S1) and [(NiL)$_2$Eu(NO$_3$)] (**2**) (Figure S2). This material is available free of charge on the Web at: http://www.csj.jp/journals/bcsj/.

References

1 a) F.-Q. Wang, X.-J. Zheng, Y.-H. Wan, C.-Y. Sun, Z.-M. Wang, K.-Z. Wang, L.-P. Jin, *Inorg. Chem.* **2007**, *46*, 2956. b) M. Yin, X. Lei, M. Li, L. Yuan, J. Sun, *J. Phys. Chem. Solids* **2006**, *67*, 1372. c) X. Yang, R. A. Jones, Q. Wu, M. M. Oye, W.-K. Lo, W.-K. Wong, A. L. Holmes, *Polyhedron* **2006**, *25*, 271. d) B. Zhao, H.-L. Gao, X.-Y. Chen, P. Cheng, W. Shi, D.-Z. Liao, S.-P. Yan, Z.-H. Jiang, *Chem.—Eur. J.* **2006**, *12*, 149. e) C. Edder, C. Piguet, J. C. G. Bünzli, G. Hopfgartner, *Chem.—Eur. J.* **2001**, *7*, 3014.

2 A. Gleizes, M. Julve, N. Kuzmina, A. Alikhanyan, F. Lloret, I. Malkerova, J. L. Sanz, F. Senocq, *Eur. J. Inorg. Chem.* **1998**, 1169.

3 a) S. Osa, T. Kido, N. Matsumoto, N. Re, A. Pochaba, J. Mroziński, *J. Am. Chem. Soc.* **2004**, *126*, 420. b) T. Hamamatsu, K. Yabe, M. Towatari, S. Osa, N. Matsumoto, N. Re, A. Pochaba, J. Mroziński, J.-L. Gallani, A. Barla, P. Imperia, C. Paulsen, J.-P. Kappler, *Inorg. Chem.* **2007**, *46*, 4458. c) J.-P. Costes, M. Auchel, F. Dahan, V. Peyrou, S. Shova, W. Wernsdorfer, *Inorg. Chem.* **2006**, *45*, 1924. d) C. M. Zaleski, E. C. Depperman, J. W. Kampf, M. L. Kirk, L. Pecoraro, *Angew. Chem., Int. Ed.* **2004**, *43*, 3912. e) A. Mishra, W. Wersdorfer, K. A. Abboud, G. Christou, *J. Am. Chem. Soc.* **2004**, *126*, 15648. f) A. Mishra, W. Wersdorfer, S. Parsons, G. Christou, E. K. Brechin, *Chem. Commun.* **2005**, 2086. g) F. Mori, T. Nyui, T. Ishida, T. Nogami, K.-Y. Choi, H. Nojiri, *J. Am. Chem. Soc.* **2006**, *128*, 1440. h) M. Ferbinteanu, T. Kajiwara, K.-Y. Choi, H. Nojiri, A. Nakamoto, N. Kojima, F. Cimpoesu, Y. Fujimura, S. Takaishi, M. Yamashita, *J. Am. Chem. Soc.* **2006**, *128*, 9008. i) S. Ueki, M. Sahlan, T. Ishida, T. Nogami, *Synth. Met.* **2005**, *154*, 217. j) F. Mori, T. Ishida, T. Nogami, *Polyhedron* **2005**, *24*, 2588. k) C. Aronica, G. Pilet, G. Chastanet, W. Wernsdorfer, J.-P. Jacquot, D. Luneau, *Angew. Chem., Int. Ed.* **2006**, *45*, 4659. l) F. Pointillart, K. Bernot, R. Sessoli, D. Gatteschi, *Chem.—Eur. J.* **2007**, *13*, 1602. m) F. He, M.-L. Tong, X.-M. Chen, *Inorg. Chem.* **2005**, *44*, 8285. n) V. M. Mereacre, A. M. Ako, R. Clérac, W. Wernsdorfer, G. Filoti, J. Bartolomé, C. E. Anson, A. K. Powell, *J. Am. Chem. Soc.* **2007**, *129*, 9248.

4 T. Yamaguchi, Y. Sunatsuki, M. Kojima, H. Akashi, M. Tsuchimoto, N. Re, S. Osa, N. Matsumoto, *Chem. Commun.* **2004**, 1048.

5 a) T. Yamaguchi, Y. Sunatsuki, H. Ishida, M. Kojima, H. Akashi, N. Re, N. Matsumoto, A. Pochaba, A. Mroziński, *Inorg. Chem.* **2008**, in press. b) T. Yamaguchi, Y. Sunatsuki, M. Kojima, H. Akashi, M. Tsuchimoto, N. Re, A. Pochaba, J. Mroziński, N. Matsumoto, PACIFICHEM 2005, Hawaii, December 15–20, **2005**.

6 T. Shiga, N. Ito, A. Hidaka, H. Okawa, S. Kitagawa, M. Ohba, *Inorg. Chem.* **2007**, *46*, 3492.

7 J.-P. Costes, F. Dahan, A. Dupuis, J.-P. Laurent, *Chem.—Eur. J.* **1998**, *4*, 1616.

8 T. Kobayashi, Y. Sunatsuki, K. Harada, T. Yamaguchi, M. Nonoyama, M. Kojima, to be submitted for publication.

9 R. D. Shannon, C. T. Prewitt, *Acta Crystallogr., Sect. B* **1969**, *25*, 925.

10 T. Yamaguchi, Y. Sunatsuki, H. Ishida, *Acta Crystallogr., Sect. C* **2008**, *64*, m156.

11 E. B. Fleischr, A. E. Gebala, D. R. Swift, P. A. Tasker, *Inorg. Chem.* **1972**, *11*, 2775.

12 We also performed the fittings taking interactions between the adjacent molecules into account. The results revealed that the intermolecular interactions are very small.

13 J.-P. Costes, F. Dahan, A. Dupuis, J.-P. Laurent, *Inorg. Chem.* **1997**, *36*, 4284.

14 Q.-Y. Chen, Q.-H. Luo, L.-M. Zheng, Z.-L. Wang, J.-T. Chen, *Inorg. Chem.* **2002**, *41*, 605.

15 O. Kahn, *Molecular Magnetism*, VCH, Weinheim, **1993**, Chap. 6.

16 M. L. Kahn, C. Mathoniere, O. Kahn, *Inorg. Chem.* **1999**, *38*, 3692.

17 a) E. B. Fleischer, A. E. Gebala, A. Levey, P. A. Tasker, *J. Org. Chem.* **1971**, *36*, 3042. b) H. Ohta, K. Harada, K. Irie, S. Kashino, T. Kambe, G. Sakane, T. Shibahara, S. Takamizawa, W. Mori, M. Nonoyama, M. Hirotsu, M. Kojima, *Chem. Lett.* **2001**, 842.

18 G. M. Sheldrick, *SHELXS97*, University of Göttingen, Germany, **1997**; SIR97: A. Altomare, M. Burla, A. Moliterni, G. Polidori, R. Spagna, *J. Appl. Crystallogr.* **1999**, *32*, 115.

19 P. T. Beurskens, G. Admiraal, G. Beurskens, W. P. Bosman, de R. Gelder, R. Israel, J. M. M. Smits, *DIRDIF99: The DIRDIF-99 program system*, Technical Report of the Crystallography Laboratory, University of Nijmegen, The Netherlands, **1999**.

20 *CrystalStructure 3.8.2., Crystal Structure Analysis Package*, Rigaku and Rigaku/MSC, The Woodlands, TX, USA, **2001–2007**.